International Journal of Coal Geology 208 (2019) 54–64

Contents lists available at ScienceDirect

International Journal of Coal Geology

journal homepage: www.elsevier.com/locate/coal

The evaluation of critical rare earth element (REE) enriched treatment solids from coal mine drainage passive treatment systems

Benjamin C. Hedin[a,b,c,*], Rosemary C. Capo[a], Brian W. Stewart[a], Robert S. Hedin[b], Christina L. Lopano[c], Mengling Y. Stuckman[c,d]

[a] Department of Geology & Environmental Science, University of Pittsburgh, Pittsburgh, PA 15260, USA
[b] Hedin Environmental, Inc., 195 Castle Shannon Blvd., Pittsburgh, PA 15228, USA
[c] National Energy Technology Laboratory, US Department of Energy, 626 Cochrans Mill Road, Pittsburgh, PA 15236, USA
[d] Leidos Research Support Team, 626 Cochrans Mill Rd, Pittsburgh, PA 15236, USA

ARTICLE INFO

Keywords:
Rare earth elements
Coal mine drainage

ABSTRACT

Rare earth elements (REE; lanthanides and Y) are essential for the development of clean energy technologies. Global demand for REE is expected to increase sharply in the coming decades, especially for certain energy-critical REE (e.g., Y and Nd), spurring investigations into novel sources of REEs. Polluted mine drainage from eastern U.S. coalfields contains elevated concentrations of dissolved Fe, Al, and Mn and is also enriched in REE by up to three orders of magnitude over unpolluted groundwater. Mine drainage remediation systems, designed to precipitate dissolved metals, can sequester > 90% of dissolved REE into the precipitated solids (treatment solids). These solids, landfilled at cost to treatment system operators, are a promising REE source. Passive treatment systems with diverse geochemical environments were sampled to determine REE mobility in these systems and REE concentrations in treatment solids. Passive treatment systems were found to produce middle and heavy REE-enriched solids, relative to the North American Shale Composite, with up to 1950 ppm REE and 55% energy-critical REE. SEM-EDS and synchrotron μ-XRF analysis demonstrate the association of REE with Mn-oxide coatings on limestone from a passive treatment system. Calculated concentration factors indicate that passive treatment systems using natural processes (e.g., drainable limestone beds and vertical flow ponds) concentrate REE into treatment solids approximately three times more effectively compared to active treatment systems using caustic chemical additions (e.g., lime). This study suggests that passive treatment systems effectively concentrate REE into treatment solids and these solids could be an alternative and more environmentally friendly source of REE compared to conventional mining on land or the seafloor. Results of this study can also aid in the design of treatment systems engineered to remove and concentrate critical REE which could provide a financial incentive to treat polluted mine water.

1. Introduction

Rare earth elements (REE), generally defined as the 15 lanthanide elements (atomic numbers 57 to 71) and yttrium, are a group of metals with similar geochemical properties and critical technological functions (Du and Graedel, 2011; USGS, 2018; Wall, 2014). REE are important components in magnets, catalysts, batteries and other products which are essential for clean energy technologies such as hybrid cars and wind turbines (Binnemans et al., 2013; DOE, 2011). The use of REE in materials critical for the manufacturing of electric cars, rechargeable batteries, and wind power infrastructure is expected to increase from 65% of total REE consumption to 92% of global REE consumption by 2030 (Zhou et al., 2017). Currently, almost 80% of worldwide REE are mined in China and REE have not been mined in the U.S. since 2016 (USGS, 2018). The importance of REE to clean energy and REE supply risk has led to the designation of five REE (Y, Nd, Dy, Eu, and Tb) as "critical resources" (DOE, 2011). The demand for certain critical REE (e.g. Nd and Dy) could increase by over 700% by 2035 with rapid green energy adoption (Alonso et al., 2012).

Current REE mining and extraction processes are associated with negative impacts to human health and the environment (Haque et al., 2014). A major concern of REE mining is the co-occurrence of REE deposits with radioactive elements like thorium and uranium, which can lead to radiological exposure during mining and processing and

* Corresponding author.
E-mail address: Bch37@pitt.edu (B.C. Hedin).

https://doi.org/10.1016/j.coal.2019.04.007
Received 29 January 2019; Received in revised form 19 April 2019; Accepted 20 April 2019
Available online 23 April 2019
0166-5162/

results in the production of radioactive waste (Ault et al., 2015; Binnemans et al., 2013; Dutta et al., 2016). Additionally, mining techniques, including open pit mining and in situ leaching, are associated with environmental impacts such as groundwater contamination, deforestation, and soil erosion (Dutta et al., 2016; Yang et al., 2013). Overall, the water and energy consumption of REE processing is significantly higher compared to other metals (Haque et al., 2014) and the environmental impact of new sources of REE, such as ocean ferro-manganese nodules, is uncertain (Hein et al., 2013; Koschinsky et al., 2018). Increasing demand for REE and environmentally costly mining/extraction techniques have sparked research into alternative sources, such as REE recovery from coal and coal related materials (Dai and Finkelman, 2018; Lin et al., 2018; Stuckman et al., 2018; Zhang and Honaker, 2018).

Acidic mine drainage (AMD), resulting from the oxidation of iron-sulfide minerals, has been shown to be enriched in REE; thus, mine drainage has been proposed as a potential source of REE (Ayora et al., 2016; Stewart et al., 2017; Ziemkiewicz et al., 2016). Contaminated mine drainage is a major global challenge facing the mining industry (Hudson-Edwards et al., 2011). In the Appalachian region of the eastern USA alone, over 5400 km of streams are polluted with mine drainage due to centuries of coal mining (EPA, 2015). Appalachian coal mine drainage (CMD) ranges from acidic (pH < 3) to circumneutral (pH ~7), anoxic to oxic, and can contain up to hundreds of mg/L of dissolved iron (Fe), aluminum (Al), and manganese (Mn) (Cravotta, 2008). Dissolved REE concentrations in Appalachian CMD range from < 1 to almost 2000 μg/L and are negatively correlated with pH (Cravotta, 2008; Stewart et al., 2017). AMD (defined here as mine drainage with pH < 5.5), in particular, is enriched in REE with total concentrations up to three orders of magnitude higher than unpolluted fresh water (Cravotta, 2008; Cravotta and Brady, 2015; Noack et al., 2014). REE can be categorized geochemically, e.g., light (La, Ce, Pr, Nd, Sm), middle (Eu, Gd, Tb, Dy, Y), and heavy (Ho, Er, Tm, Yb, Lu), or by application, such as energy-critical (Y, Nd, Dy, Eu, Tb) (DOE, 2011; Seredin and Dai, 2012). Based on a survey of the literature, (Cravotta, 2008; Cravotta and Brady, 2015; Stewart et al., 2017), Appalachian CMD is enriched in both energy critical (55% ± 12 wt% of total REE concentrations) and middle REE and depleted in light REE when normalized to the North American Shale Composite (NASC) (Gromet et al., 1984; Haskin and Haskin, 1966).

Mine drainage treatment involves acid neutralization and/or redox adjustment to precipitate dissolved metals, resulting in large quantities of waste solids ($> 1.6 \times 10^7$ kg/year in Pennsylvania, USA alone Stream Restoration, I (2018)), the disposal of which is a major cost to treatment operators (Cavazza and Beam, 2010; Cravotta and Brady, 2015). These precipitated solids, defined herein as treatment solids, are enriched in total REE up to ~1000 ppm (Stewart et al., 2017) and have been proposed as a potential source of REE (Ayora et al., 2016; Erickson, 2018; Stewart et al., 2017; Zhang and Honaker, 2018; Ziemkiewicz et al., 2016). Estimates indicate that up to 5×10^5 kg of REE could be recovered every year from Appalachian CMD alone (Stewart et al., 2017). However, the impact of treatment methods on REE concentrations in treatment solids is not well documented.

Mine drainage treatment technologies generally fall into one of two categories: “active treatment” or “passive treatment” (Younger et al., 2002). Active treatment systems involve the constant addition of chemicals (e.g., lime, sodium hydroxide, and hydrogen peroxide) to neutralize acidity and oxidize and/or hydrolyze dissolved metals. Active systems require delivery, storage, and mixing procedures for chemical reagent(s), routine maintenance of mechanical equipment, and electricity for pumps and aerators (Younger et al., 2002). Treatment solids (Fe, Al, and Mn oxides and hydroxides as well as other minerals such as calcite, dolomite, and gypsum) plus unreacted caustic agents accumulate as sludge in settling ponds or mechanical clarifiers which must be regularly cleaned.

Passive treatment systems typically do not use electricity or chemicals, and rely on gravity flow, natural geochemical processes, and microbial activity (Hedin et al., 1994; Younger et al., 2002). There are many different passive treatment technologies and each technology is applied to specific water chemistry (Hedin et al., 2013; Skousen et al., 2017). Limestone aggregate is commonly used in passive systems to raise the pH to 6–8, which results in a bicarbonate-buffered solution that facilitates the oxidation, hydrolysis, and precipitation of dissolved Fe, Al, and Mn, and largely limits the precipitation of nontarget solids (e.g., calcite, gypsum, $Mg(OH)_2$).

Unlike active systems, which typically produce a single sludge containing a mixture of metal precipitates and unreacted chemical additives, passive systems often treat CMD sequentially in separate treatment steps. Sequential treatment technologies can generate different metal-rich solids at each step and may provide different geochemical and physical environments for REE enrichment. Examining the processes and conditions that facilitate REE precipitation and selective enrichment in passive treatment systems offers the opportunity to maximize REE recovery in treatment solids.

The composition of treatment solids in passive treatment systems can be influenced by pH, redox, and precipitation mechanics. For example, the removal of dissolved oxygen (DO) via microbial respiration in an organic substrate layer preceding a limestone bed limits Fe(II) and Mn(II) oxidation in the limestone bed, but allows for Al(III) hydrolysis (Hedin et al., 2010). In subsequent oxidizing conditions, the rapid oxidation of Fe(II) at near-neutral pH can produce solids composed predominantly of Fe(III) hydroxide. Additionally, the heterogeneous precipitation of Mn(II) via sorption and autocatalytic/biologically-catalyzed oxidation of Mn(II) on existing Mn(III/IV) oxide results in a growing, armored Mn-oxide surface on limestone solids that is largely immobile (Hansel et al., 2012; Luan et al., 2012; Post, 1999; Santelli et al., 2011; Tan et al., 2010). Homogenous Al(III) hydroxide precipitation via hydrolysis often creates colloidal solids that can be transported by turbid water (Hedin Environmental, 2008). Phases in passive mine drainage treatment solids include amorphous Al phases (e.g., $Al(OH)_3$ and $Al(OH)(SO_4)$) (Ayora et al., 2016; Cravotta and Trahan, 1999; Pu et al., 2010), iron oxides and hydroxides (e.g., goethite, FeO(OH); ferrihydrite, $Fe(OH)_3{\cdot}0.5H_2O$; and schwertmannite, $Fe_8O_8(OH)_6(SO_4)$) (Bigham et al., 1996; Cravotta and Trahan, 1999; Hedin, 2003; Kairies et al., 2005), and manganese oxides (e.g., birnessite, $(Na,Ca)Mn_7O_{14}$; and todorokite $(Ca,Na,K)_xMn_6O_{12}$) (Cravotta and Trahan, 1999; Tan et al., 2010).

Although Cravotta and Brady (2015) documented REE removal in active and passive CMD treatment systems, REE behavior in different types of passive mine drainage treatment systems is largely unknown. Work in other geochemical environments suggests that dissolved REE can be removed by adsorption on hydrous Fe(III) oxides/hydroxides at neutral pH (e.g. goethite and ferrihydrite), but are not removed by Fe(III) oxides/hydroxides at low pH (e.g. schwertmannite) (Ayora et al., 2016; Bau, 1999; de Carlo et al., 1998; Prudêncio et al., 2015; Verplanck et al., 2004). Ayora et al. (2016) used sequential extractions and synchrotron micro-x-ray fluorescence (μ-XRF) on treatment solids from benchtop experiments simulating passive treatment systems to show the sorption and co-precipitation of REE on basaluminite (aluminum-sulfate mineral) treatment solids. Zhang and Honaker (2018) titrated AMD with NaOH in a stepwise manner, collected precipitated solids after each NaOH addition step, and found that REE were most enriched in the Al solids. Mn oxides (e.g. birnessite and todorokite) can also be produced in passive treatment systems (Cravotta and Trahan, 1999; Tan et al., 2010). Mn oxides exhibit strong sorptive properties (Bau et al., 1996a; Cao et al., 2001); however, to-date, the role of Mn oxides in REE removal from mine drainage has not been investigated.

To investigate the REE characteristics in treatment solids, we designed this study to: (1) determine REE mobility in geochemically diverse passive treatment systems and identify treatment solids that are enriched in REE, and (2) evaluate how different mine drainage treatment technologies concentrate REE into treatment solids. To do this, we

Table 1
Summary of passive treatment systems sampled in this study and the major geochemistry of the untreated water and conditions found inside the treatment systems (internal pH).

Treatment system	Samples	Influent pH[a]	Internal pH[a]	Internal redox[b]	Major pollutants
Settling ponds					
SP-1	Solids	Circumneutral	Circumneutral	Oxic	Fe
Low pH Fe oxidation					
LP-1	In/Out, solids	Low	Low	Oxic	Fe, Al, Mn
Vertical flow ponds					
VFP-1	In/Out	Low	Circumneutral	Anoxic	Fe, Al, Mn
VFP-2	In/Out	Low	Circumneutral	Anoxic	Fe, Al, Mn
Drainable limestone beds					
DLB-1	In/Out, solids	Low	Circumneutral	Oxic	Al
DLB-2	In/Out, solids	Low	Circumneutral	Oxic	Al, Mn
DLB-3	In/Out	Low	Circumneutral	Oxic	Fe, Al, Mn
DLB-4	Solids	Low	Circumneutral	Oxic	Fe, Al, Mn

[a] Low pH is between 2.9 and 4.1 and circumneutral pH is between 6.3 and 7.2.
[b] Oxic is between 2.3 and 13 mg/L DO and Anoxic is between 0.1 and 0.6 mg/L DO.

investigated REE attenuation in treatment solids from selected passive treatment systems and documented the physical and geochemical conditions that lead to accumulation of high concentrations of REE. Second, we mapped micro-scale REE distribution and their associations with different phases in Mn rich treatment solids recovered from a passive treatment system. Third, we calculated REE concentration factors for 17 passive and active treatment systems. The results of this study will help inform future REE recovery efforts and aid in the construction of treatment systems specifically designed to remove and concentrate REE from CMD. They also have the potential to support environmentally friendly CMD remediation efforts, often spearheaded by local community groups, with REE resource recovery.

2. Methods

2.1. Treatment system sampling

Influent (untreated) and effluent (treated) water samples and treatment solid samples were collected from four passive treatment technologies each with unique internal geochemical conditions (Table 1). The passive treatment technologies sampled in this study are oxidation/settling ponds (SPs), low pH Fe removal (LP) systems, vertical flow ponds (VFPs), and drainable limestone beds (DLBs). Different sites using the same treatment technology are identified numerically after the treatment technology (e.g., VFP-1, VFP-2…etc.).

The SP-1 treatment system consists of a series of six settling ponds and a wetland, treating circumneutral, anoxic CMD with elevated Fe(II) concentrations. Passive aeration generates oxic, circumneutral geochemical conditions, promoting abiotic Fe(II) oxidation and the settling of Fe(III) solids (Fig. 1A; Table 1) (Hedin, 2008). Treatment solids were collected from each setting pond and the wetland.

The LP-1 treatment system consists of an open channel treating low pH, oxic CMD with elevated Fe, Al, and Mn concentrations. The generation of oxic, low pH conditions through the system promotes biotic Fe(II) oxidation and the settling of Fe(III) solids (Fig. 1B; Table 1) (Stream Restoration, I, 2018). Influent and effluent water samples and treatment solids were collected from LP-1 for analysis.

The VFP-1 and VFP-2 treatment systems are limestone beds covered with organic substrate and standing water treating low pH, oxic CMD with elevated Fe, Al, and Mn concentrations (Fig. 1C; Table 1). Microbial aerobic respiration in the organic substrate creates anoxic conditions and reduces Fe(III) to Fe(II) before reacting with the limestone. This limits the oxidation and precipitation of dissolved Fe and Mn; but allows for the hydrolysis and precipitation of dissolved Al (Hedin et al., 2010). Influent and effluent water samples were collected from VFP-1 and VFP-2, but treatment solids were not available for sampling.

The DLB-1, DLB-2, DLB-3, and DLB-4 treatment systems are limestone beds treating low pH, oxic CMD with elevated Fe, Al, and Mn concentrations (Fig. 1D; Table 1). Limestone dissolution neutralizes acidity and generates alkalinity, promoting the precipitation of dissolved Fe, Al, and Mn via oxidation and hydrolysis reactions. DLBs are periodically drained of fluid (approximately weekly) to remove solids that have accumulated in the limestone. Draining removes Al, but not Mn solids, from the limestone bed into settling ponds. Mn precipitants tend to cement onto the limestone aggregate and are not removed with draining (Hedin Environmental, 2008). Influent and effluent water samples were collected from DLB-1, DLB-2, and DLB-3. Solid samples were collected from the flush pond of DLB-1, the flush pond and limestone bed of DLB-2, and the limestone bed of DLB-4.

2.2. Chemical analysis

Fourteen influent and effluent water samples from the passive treatment systems described above were collected and filtered to < 0.45 μm. Acidified aliquots of the samples (2% ultrapure nitric acid) were analyzed for major elements, trace elements, and all REE at Activation Laboratories, Ontario, Canada (Actlabs, 2018) by inductively coupled plasma mass spectrometry (ICP-MS) (6 - Hydrogeochemistry-ICP/MS method). Unacidified aliquots were analyzed for anions by ion chromatography (IC) (6B - Ion Chromatography method). Sulfate concentrations were measured at G&C Coal Analysis Labs, Summerville, PA, USA by IC. Cation-anion balances are ≤ ± 6% except for LP-1 influent and effluent which are −24% and − 21% imbalanced, respectively. Field data collected concurrently included flow rate, pH, conductivity, dissolved oxygen, oxidation-reduction potential, and alkalinity. Alkalinity was measured via gran titrations on unfiltered samples collected with minimal headspace no > 10 h after collection.

Approximately 3 l of treatment solids collected from the five passive treatment systems described above were stored in resealable plastic bags until processing. Solid samples were dried at 105 °C and when treatment solids were cemented onto limestone, the limestone aggregate was dried and lightly sieved to < 2 mm to separate the limestone and cemented solids. For DLB-1, DLB-2, and DLB-4, dried treatment solids were analyzed for major oxides, trace elements, and all REE at Activation Laboratories by lithium metaborate/tetraborate fusion and inductively coupled plasma optical emission spectrometry (ICP-OES) and ICP-MS (4Litho method) and for C and S by infrared spectroscopy (IR) (4F - C, S method) (Actlabs, 2018). Each individual REE was quantified on at least 4 certified reference materials (CRMs) and average deviations for individual lanthanide elements were < 4% and for Y was 14%. For SP-1, dried treatment solids were analyzed for major oxides, trace elements, and select REE (Y, La, Ce, Nd, Sm, Eu, Tb, Yb, and Lu) at Activation Laboratories by ICP-OES and instrumental neutron activation analysis (INAA) (4E-expl. method) (Actlabs, 2018). Due to incomplete REE analysis and many REE concentrations below the method detection limit, Y concentrations are used as proxies for total REE concentrations at SP-1 using the linear regression calculated in this study (Total REE (μg/L) = Y (μg/L) × 3.6875; R^2 = 0.76; Fig. S1).

Major element data for solids in this study are reported as oxides as measured by Activation Labs (e.g., Fe_2O_3) which does not reflect the mineralogy of the solids in treatment systems (e.g., FeO(OH)). Loss on ignition (LOI) is the mass of volatiles (e.g. hydrates, carbon dioxide from carbonates, and organic matter) lost from a sample heated to 750 °C (Actlabs, 2018). Total recovery (major oxides + LOI + C + S)

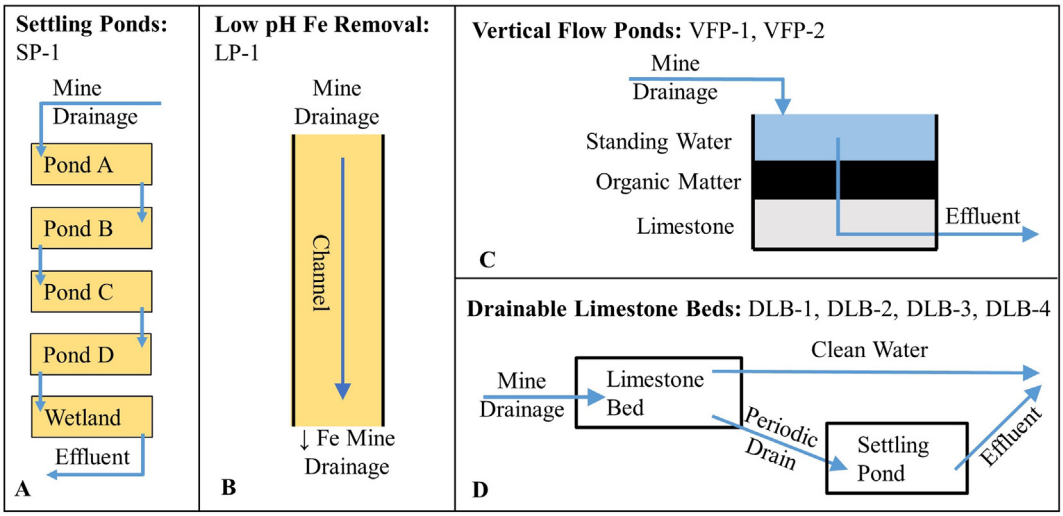

Fig. 1. Schematics of passive treatment systems sampled in this study. A. sequential settling ponds (SP) and wetlands. B. low pH Fe removal system (LP). C. vertical flow pond (VFP). D. drainable limestone bed (DLB).

ranges from 96% to 103% for the solid samples in this study.

2.3. Microanalysis

Powdered treatment solids collected from DLB-2, and − 4 were analyzed for crystalline solids via X-ray diffraction (*XRD*). Ground material was backloaded into a 10 mm diameter cavity spin mount for analysis via XRD. The samples were run on a PANalytical X'Pert Pro utilizing copper X-rays at 45 kV, 40 mA, with an X'Celerator parallel plate detector. The samples were scanned between 4 and 70° 2θ at using a step size of 0.033°/step and a 1000 s count time. The resulting XRD patterns were compared against the PDF-4 ICDD database using the X'Pert HighScore program to identify the crystalline mineral phases present.

A cross-section of a single piece of Mn-coated limestone from DLB-2 was prepared into a 30-μm thick doubly-polished microprobe-prepped thin section (Spectrum Petrographics, Inc.) for Scanning Electron Microscopy (*SEM*) imaging and synchrotron micro-X-ray Fluorescence (*μ-XRF*) elemental maps. SEM with energy dispersive X-ray spectroscopy (SEM-EDS; Quanta 600 FEG, FEI, Hillsboro, OR) was performed for point-analysis and mapping selected regions in BSE mode (under high vacuum, 20 keV excitation energy, with 3.0 μm spot size). μ-XRF mapping was conducted using synchrotron radiation at beam line 2–3 at the Stanford Synchrotron Radiation Light Source (SSRL) which was equipped with a 4-μm beam size, Si(1,1,1) crystal, and a single element Si Vortex detector. Mapping was conducted at 9500 eV with a 5 μm step size and 100 ms dwell time. Element maps were processed in the SIXpack software (Webb, 2005) including using PyMCA fitting to deconvolute and potential spectral interferences between REE and transition metals, as per Stuckman et al. (2018).

2.4. REE concentration in different treatment systems (passive vs. active)

To evaluate how efficiently REE are concentrated into treatment solids by different treatment technologies, treatment solid and influent CMD chemistry from 17 individual treatment systems were paired and analyzed. Solids data are from this study, Hedin Environmental, and Stewart et al. (2017). Solids collected by Hedin Environmental were analyzed by Activation Laboratories. Data from multiple solid samples from a single treatment system were averaged. Influent CMD data are from this study, Cravotta (2008), and Cravotta and Brady (2015).

From these data, solids concentration factors for each treatment system were calculated. Yttrium concentrations were used as proxies for total REE concentrations in both solids and influent CMD samples because for some samples, either Y was the only REE measured or most REE are below detection limits. Total REE concentrations calculated from Y concentrations are noted in the text and figures.

Concentration factors can be calculated using REE concentrations in treatment solids and influent CMD (Ziemkiewicz et al., 2016). However, REE concentrations in a treatment solid sample are a composite value representing accumulation over time, while REE concentrations in an influent CMD waters are an instantaneous value and subject to diel and seasonal fluctuations and dilution. We propose to account for this difference by normalizing dissolved REE concentrations (using Y as a proxy) to total dissolved solids (TDS) in influent CMD. This normalization accounts for the effects of dilution and diel cycling because of the expected covariance of dissolved REE and TDS at a given CMD discharge (Vesper and Smilley, 2010). We calculate the REE solids concentration factor (CF_s) for individual treatment systems as:

$$CF_s = \frac{Y_{ts}}{Y_{in}/TDS_{in}}$$

where Y_{ts} (ug/g) is the yttrium concentration in the treatment solids, Y_{in} (μg/L) is the concentration in the influent, and TDS_{in} (g/L) is the total dissolved solids of the influent.

3. Results

3.1. REE partitioning in passive treatment systems

Settling ponds (SPs) treat circumneutral mine drainage with elevated Fe concentrations by oxygen transfer and CO_2 degassing to promote the abiotic oxidation of Fe(II) (Younger et al., 2002). SP-1 influent has high Fe (58 mg/L) and low REE (6 μg/L) concentrations at the influent and the circumneutral and oxic conditions decrease Fe concentrations to < 0.1 mg/L in the effluent (Table 2). Fe(III) hydroxide/oxides constitute approximately 70% of the settling pond solids (Fig. 2), likely as goethite/ferrihydrite (Kairies et al., 2005).

Total REE concentrations in SP-1 treatment solids were calculated from Y concentrations because the concentrations of some REE were below the method detection limit and because Y concentrations and total REE concentrations are well correlated (Fig. S1). REE concentrations in the solids are 380 ppm in the first pond and decrease to 37 ppm by the seventh pond (Fig. 2). REE concentrations in the treatment solids are relatively low in this system due to low influent REE concentrations (Table 2).

Low-pH Fe removal systems (LPs) treat low pH mine drainage with

Table 2
Influent and effluent chemistry of treatment systems in this study. For SP-1, major element data are from Hedin Environmental and REE data are from Cravotta, 2008. DLB 4 data are from Hedin Environmental. All other data were collected in this study. HCO_3^- is calculated from field alkalinity.

Site	Location	Flow	pH	DO	HCO_3	Fe	Al	Mn	Ca	Mg	Na	K	SO4	Cl	Si	Sr	ΣREE	TRT
		L/s								mg/L							µg/L	hours
SP-1	Influent	115.9	6.31	0.7	416	58.3	< 0.1	1.0	154	41	479.1	6.1	1105	124.7	9.7	2.2	6	71
SP-1	Effluent		7.93	18.8	278	< 0.1	< 0.1	0.1	130	41	456.0	4.7	1057	140.5	5.4	1.9	N/A	
LP-1	Influent	0.9	2.86	6.4	0	128.9	32.3	43.1	122	98	28.4	6.4	2077	47.2	12.9	0.2	1297	21
LP-1	Effluent		2.94	13.0	0	61.8	25.8	37.2	168	88	24.0	6.1	1718	39.6	10.3	0.3	1003	
VFP-1	Influent	0.3	4.13	3.1	0	64.4	40.1	67.8	158	234	3.5	7.5	1759	2.5	18.9	0.2	779	103
VFP-1	Effluent		6.28	0.6	242	32.4	0.6	*79.8	403	295	4.1	8.6	2329	2.8	6.0	1.3	73	
VFP-2	Influent	6.0	2.73	10.9	0	14.0	17.2	3.8	18	21	0.7	1.2	364	0.4	11.2	0.1	145	201
VFP-2	Effluent		6.84	0.0	171	4.1	< 0.1	3.1	158	17	0.7	1.5	354	0.5	9.4	0.2	1	
DLB-1	Influent	0.2	3.27	4.7	0	0.7	19.7	0.8	106	45	11.7	0.8	608	4.9	16.9	1.2	181	119
DLB-1	Effluent		6.62	4.2	274	< 0.1	0.1	0.1	252	47	11.7	1.0	560	5.6	12.2	1.5	5	
DLB-2	Influent	2.7	3.91	3.9	0	0.0	7.4	16.1	91	99	2.8	4.4	701	0.9	10.4	0.1	151	31
DLB-2	Effluent		6.98	3.2	209	< 0.1	< 0.1	0.3	193	100	2.8	4.4	713	1.3	9.1	0.2	3	
DLB-3	Influent	0.6	3.35	12.1	0	5.6	4.0	40.3	422	273	4.0	8.0	1997	15.6	12.9	1.3	453	94
DLB-3	Effluent		7.24	2.3	111	0.2	0.1	0.1	496	264	0.1	7.9	1868	21.2	11.4	3.1	11	
DLB-4	Influent	0.1	2.99	N/A	0	4.0	16.8	7.3	N/A	N/A	N/A	N/A	394	N/A	N/A	N/A	N/A	54
DLB-4	Effluent		7.36	N/A	124	< 0.1	< 0.1	0.3	N/A	N/A	N/A	N/A	392	N/A	N/A	N/A	N/A	

TRT = theoretical retention time. N/A = data not available.
* Effluent Mn concentration is likely greater than influent because of changing influent water chemistry in one bed volume.

elevated Fe concentrations by oxygen transfer to promote the biotic oxidation of Fe(II) (DeSa et al., 2010; Larson et al., 2014). The low pH and oxic conditions in LP-1 decrease dissolved Fe from 129 mg/L in the influent to 62 mg/L in the effluent (52% reduction). Concentrations of REE and other dissolved metals, as well as pH, are generally conserved through the treatment system, with total REE concentrations only decreasing from 1297 µg/L to 1003 µg/L, a 23% reduction (Table 2). Approximately 50% of the change in REE concentration is likely due to dilution from unpolluted fresh water, as indicated by the similar decreases in Mn, Na, Cl, and K concentrations (Table 2), which should act as conservative tracers under low pH conditions. Accounting for this dilution, only 11% of dissolved REE and 45% of dissolved Fe is removed in LP-1 (Fig. 3).

Solids accumulating in the open channel of LP-1 are 67% Fe(III) oxides/hydroxides (Fig. 2) with both amorphous Fe mineral and goethite phases (Fig. S2). Based on the low pH and high SO_4 concentration in LP-1, schwertmannite is likely precipitating (Bigham et al., 1996) and recrystallizing to goethite over months/years (Schwertmann and Carlson, 2005). These solids contain 24 ppm REE (Fig. 2) and have a flat REE pattern when normalized to NASC (Fig. 4). The treatment solids produced at LP-1 contain low concentrations of REE (Fig. 2) despite high dissolved REE concentrations in the influent (Table 2).

Vertical flow ponds (VFPs) treat low pH CMD with elevated Fe, Al, and/or Mn concentrations by microbial respiration and limestone dissolution. Microbial aerobic respiration in an organic substrate removes DO to limit dissolved Fe(II) and Mn(II) oxidation and precipitation in limestone, maintaining the reactivity and porosity of the limestone (Hedin et al., 2013). DO concentrations and pH values in VFP-1 and VFP-2 effluent were 0.6 mg/L and 0.1 mg/L, and 6.3 and 6.8, respectively (Table 2). Therefore, the aqueous geochemical conditions in the limestone layer of these sites are anoxic/suboxic and circumneutral.

When effluent concentrations are normalized to influent concentrations, VFP-1 and -2 remove an average of 60% Fe, 99% Al, 9% Mn, and 95% total REE (Table 2) with lower Y removal relative to other REE (Fig. 3). Treatment solids were not available for sampling from VFP-1 and -2 so total REE concentrations in the VFP treatment solids were estimated using a mass balance approach. This calculation assumed Fe, Al, Mn, and Si was removed (influent minus effluent) as goethite (FeO(OH) (Kairies et al., 2005), Al hydroxide sulfate (Al(OH)(SO_4) (Pu et al., 2010), birnessite (MnO_2) (Cravotta and Trahan, 1999; Tan et al., 2010), and silica (SiO_2), respectively, and 30% LOI (average from all treatment solids measured in this study). To evaluate the accuracy of this calculation, identical calculations using influent and effluent data from two other treatment systems sampled in this study were compared to total REE concentrations measured by lab analysis. Calculated and measured values from these two treatment systems agreed to within 15%. Calculated REE concentrations in treatment

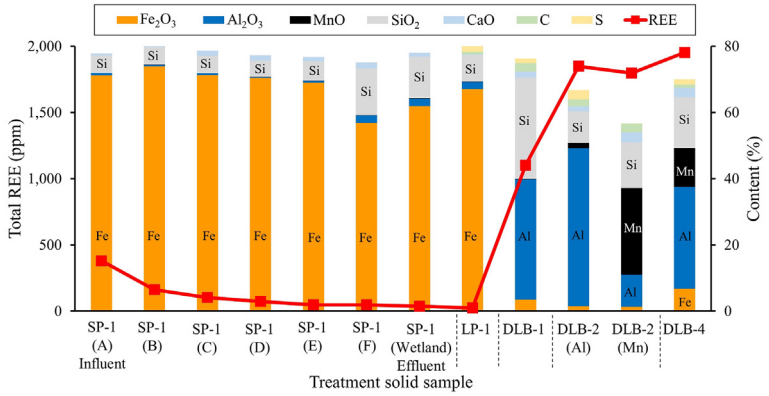

Fig. 2. Total REE and oxide concentrations of the treatment solids collected from passive treatment systems in this study. The remaining solids composition (> 2%) is loss on ignition (LOI). SP-1 total REE concentrations are calculated from Y concentrations and do not include C and S measurements.

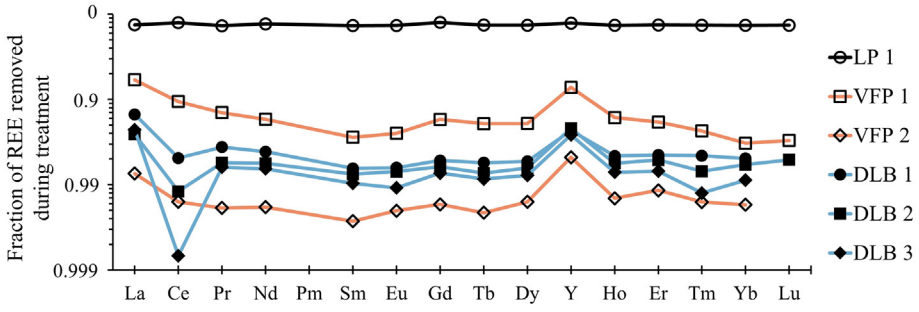

Fig. 3. Fraction of total REE removal for DLBs (in blue), VFPs (in red), and LPs (in black). Removal is calculated as (1 – $REE_{effluent}$ / $REE_{influent}$). Redox conditions are reducing in VFPs and oxidizing in DLBs and LP. Missing data for Lu is due to effluent samples below detection limit (< 0.004 µg/L). (For interpretation of the references to colour in this figure legend, the reader is referred to the web version of this article.)

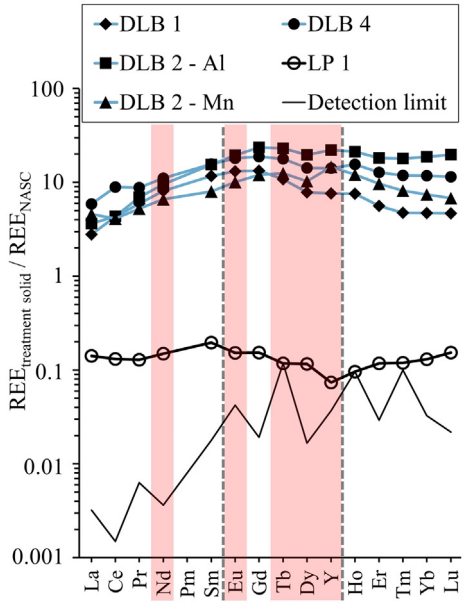

Fig. 4. REE concentrations in treatment solids normalized to NASC REE concentrations. Vertical dashed lines divide light REE (left), middle REE (center), and heavy REE (right). Energy critical REE are highlighted in pink. The solid line is detection limits normalized to NASC. (For interpretation of the references to colour in this figure legend, the reader is referred to the web version of this article.)

solids are noted in the text and figures. Calculated REE concentrations in the precipitated solids of VFP-1 and VFP-2 are ~1500 and ~800 ppm, respectively.

Drainable limestone beds (DLBs) treat low pH CMD with dissolved Fe, Al, and/or Mn by calcite dissolution (Hedin et al., 2013). The limestone beds are open to the atmosphere, and dissolved Fe, Al, and Mn are precipitated via oxidation and hydrolysis reactions within the limestone. DO concentrations and pH values in the effluents of DLB-1, DLB-2, and DLB-3 indicate that the geochemical conditions within the limestone bed are circumneutral and oxic (Table 2). When effluent concentrations are normalized to influent concentrations, DLB-1, −2, and − 3 remove an average of 95% Fe, 99% Al, 97% Mn, and 98% REE (Table 2) and preferentially remove Ce relative to other REE (Fig. 3). Like VFPs, the DLBs also show less removal of Y relative to other REE (Fig. 3).

DLBs are periodically drained empty to remove solids to maintain limestone porosity and reactivity (Hedin et al., 2013). The turbid conditions created by rapidly draining DLBs removes Al solids from the limestone bed to a settling pond but does not remove Mn solids which are armored onto the limestone aggregate. Treatment solids collected from the flush basins at DLB-1 and DLB-2 are 36% and 38% Al_2O_3 and contain 1103 and 1849 ppm REE, respectively (Fig. 2). Mn-rich coating material physically removed from the limestone at DLB-2 contains 26% MnO and 1798 ppm REE, after subtracting out the contribution of co-extracted limestone (based on elevated C and CaO content and calcite in XRD patterns) (Fig. 2; Fig. S2). Treatment solids coating the limestone at DLB-4 contain 7% Fe_2O_3, 31% Al_2O_3, 12% MnO, and 1952 ppm REE with negligible limestone content (Fig. 2). When normalized to NASC, all DLB treatment solids are light REE depleted and do not contain REE anomalies (Fig. 4). On a mass basis, DLB treatment solids average 44% middle and heavy REE and 48% critical REE.

3.2. Mineralogy and advanced imaging

XRD analysis of treatment solids suggest that the solid phases are largely amorphous (Fig. S2), with minor trace crystalline components (e.g. quartz and calcite), that do not match the overall bulk chemistry of the solids (e.g. Fe-, Al-, or Mn-rich) described in Fig. 2. The amorphous or poorly-crystalline nature of the treatment solids in this study are consistent with previous XRD analyses of treatment solids from passive CMD treatment systems (Cravotta and Trahan, 1999; Kairies et al., 2005; Pu et al., 2010; Tan et al., 2010).

SEM and synchrotron µ-XRF analyses of a CMD passive treatment system solid from this study show a strong correlation between REE and Mn phases. A photo-scan of the cross section of a piece of limestone aggregate from DLB-2 reveals a black coating on the surface of the limestone (Fig. 5A). SEM-BSE imaging further demonstrates that the

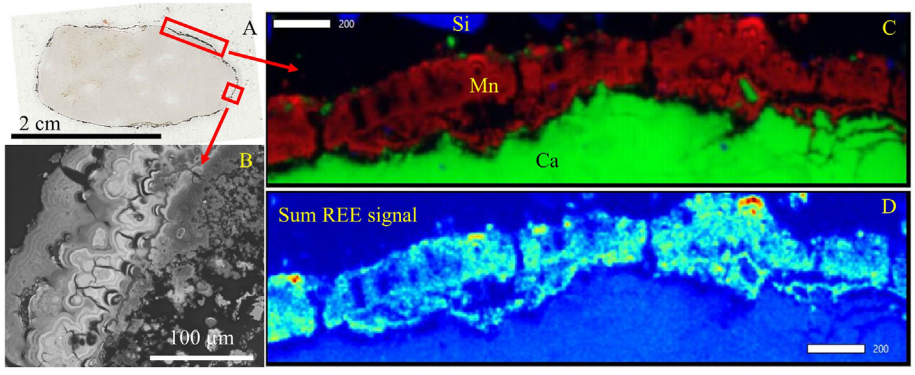

Fig. 5. A. Photo-scan of a thin section from cross section of limestone from DLB-2. B. SEM-EDS image of the Mn coating showing botryoidal morphology. C. Tri-colored µ-XRF map collected at an excitation energy of 9500 eV, 5 µm step size and 100 msec dwell time with Ca in green, Mn in red, and Si in blue showing Mn accumulating on the edge of the limestone. D. µ-XRF REE map (sum of La, Ce, Nd, Sm, Eu, Gd, Dy, Yb, and Lu counts from PyMCA fitting) with same mapping region as C. The colour scale from blue to red represents low to high photon counts. Scale bars in C and D are 200 µm. (For interpretation of the references to colour in this figure legend, the reader is referred to the web version of this article.)

limestone coating is Mn-rich with botryoidal morphology; an identifying characteristic of Mn oxides and ocean ferro-manganese nodules (Hein et al., 2013; Margolis and Burns, 1976; Post, 1999) (Fig. 5B). EDS analysis of the Mn-rich coating via SEM does not detect the presence of REE in this surface coating; however, synchrotron μ-XRF mapping captures the 200–300 μm thick Mn-rich coating on the limestone surface (Fig. 5C) and the co-localization of REE in those coatings (Fig. 5D).

4. Discussion

4.1. REE behavior in passive treatment systems

The results presented in this study confirm that the removal of dissolved REE from CMD is pH dependent. Low pH Fe removal technology that maintains pH < 3.0 (e.g. LP-1) removes 12% of dissolved REE from AMD (Fig. 3). Vertical flow pond (VFP) and drainable limestone bed (DLB), passive treatment technologies that raise pH to > 6.0 using limestone dissolution, removed > 90% of dissolved REE from AMD (Fig. 3), which is corroborated by data from other systems as well (Cravotta and Brady, 2015).

The near complete removal of dissolved REE both in anoxic and oxic conditions in VFPs and DLBs, respectively, suggests that dissolved REE removal occurs under a range of redox conditions (Table 2; Fig. 3). In addition to field DO measurements (Table 2), the presence or absence of preferential Ce removal can be used as a proxy for the redox conditions in treatment systems (Fig. 3). Ce is redox sensitive and may oxidize and hydrolyze from $Ce(III)_{(aq)}$ to $Ce(IV)O_{2(s)}$ in circumneutral, oxic environments (Bau and Koschinsky, 2009). Preferential Ce removal in DLBs (Fig. 3) suggest that Ce is oxidized and hydrolyzed and that the geochemical conditions in DLBs are circumneutral and oxic. Iron and/or manganese oxides, present in DLB-2 and DLB-3, can scavenge Ce and oxidize Ce(III) to Ce(IV) (Bau and Koschinsky, 2009; Ohta and Kawabe, 2001). The absence of preferential Ce removal in VFPs (Fig. 3) is consistent with anoxic geochemical conditions that prevent the oxidation of Ce(III).

The presence of organic matter in VFPs could also indicate that organic complexes are important in these systems. Humic acid-REE complexes can suppress Ce anomalies even in the presence of Mn and Fe oxides (Davranche et al., 2004; Davranche et al., 2008). Additionally, REE can bind to humic acid at pH < 4 (Pourret and Martinez, 2009) suggesting REE could be removed in the organic matter portion of VFPs. Additional work on the distribution of REE in VFPs, such as detailed sampling of VFP substrate and/or sequential extractions, will be important to determine where REE accumulate in these systems.

The anomalously low Y removal observed in both DLBs and VFPs has been seen in REE sorption studies in seawater (Bau, 1999; Bau et al., 1996b) and mine drainage (Vesper and Smilley, 2010). This phenomenon is poorly understood but may be due to the weak surface complexation of Y (Bau and Koschinsky, 2009).

The pH dependent removal of REE from AMD in a range of redox conditions could be used to improve the design of treatment systems optimized to remove REE from solution. For example, circumneutral, anoxic conditions could be used to promote the removal of redox-insensitive metals (e.g. REE and Al), and limit the removal of redox-sensitive metals (e.g. Fe and Mn).

4.2. REE in treatment solids

Setting pond (SP) systems do not create treatment solids with high REE concentrations (Fig. 2) because this technology is primarily used to treat circumneutral mine drainage with low dissolved REE (Table 2) (Hedin et al., 2013). Previous studies have shown that REE are rapidly adsorbed or co-precipitated by Fe(III) hydroxides (e.g. goethite and ferrihydrite) in circumneutral conditions (Bau, 1999; de Carlo et al., 1998; Verplanck et al., 2004); similar to the geochemical conditions in SP-1. In this study, REE concentrations in treatment solids from SP-1 are highest near the influent of the systems and decrease through the system. This suggests REE are rapidly removed with Fe(III) hydroxides at circumneutral pH (Fig. 2) and is consistent with their adsorption by goethite (Liu et al., 2017; Verplanck et al., 2004). Therefore, any potential REE recovery from SP treatment solids should be targeted near the influent of these systems where pH increases rapidly owing to CO_2 outgassing and, correspondingly, Fe(II) oxidation and Fe(III) accumulation take place (Cravotta and Brady, 2015).

Low pH Fe removal (LP) systems do not produce treatment solids with high REE concentrations (Fig. 2) because dissolved REE are not removed from AMD in these systems (Fig. 3). This is consistent with previous studies showing both synthetic (Bau, 1999; de Carlo et al., 1998) and natural (Verplanck et al., 2004) Fe(III) hydroxides precipitated at low pH (e.g. schwertmannite) do not remove dissolved REE from solution. Thus, treatment solids from LP systems should not be targeted for REE recovery. However, these systems could be used as a pre-treatment to remove dissolved Fe for subsequent downstream REE recovery using co-precipitation of REE with other dissolved metals (Al and Mn). For example, LP-1, increases the REE/Fe ratio by 61% by removing 45% Fe but only 11% REE (Table 2). Increasing retention time in the systems could remove more Fe and further increase the REE/Fe ratio.

Vertical flow pond (VFP) and drainable limestone bed (DLB) systems create treatment solids with high REE concentrations that could be targeted for REE recovery (Fig. 2). In the circumneutral, anoxic geochemical conditions characteristic of VFPs, there is limited removal of redox-sensitive metals, such as Fe and Mn, and near complete removal of dissolved REE and Al from solution (Table 2; Fig. 3), producing treatment solids with high REE concentrations. In the circumneutral, oxic geochemical conditions characteristic of DLBs, there is near complete removal of Fe, Al, Mn, and REE (Table 2; Fig. 3), and both Al- and Mn-rich treatment solids are enriched in REE.

Aluminum hydroxides formed in mine drainage environments have been reported to sequester REE in previous studies (Ayora et al., 2016). Synchrotron μ-XRF from this study reveal that REE can also be associated with Mn solid phases in CMD treatment solids produced from DLB passive treatment systems (Fig. 5). The REE enrichment is not associated with specific mineral grains (e.g., monazite) that have been identified in other novel REE sources such as coal fly ash (Montross et al., 2018; Stuckman et al., 2018; Zhang and Honaker, 2018). Along with the non-crystalline nature of the Mn oxides, this suggests that REE are diffusely distributed in the Mn-rich treatment solids cemented onto aggregate in DLB-2. However, the exact removal processes of REE by Mn and Al compounds by surface sorption or solid-solution substitution into the mineral structure remains unclear. In marine systems, REE are associated with Fe and Mn oxide phases in ocean ferro-manganese nodules (Bau and Koschinsky, 2009) and likely accumulate on these solids via surface complexation (Bau et al., 1996b). Additional microanalysis work on the associations between REE and geochemically diverse treatment solids will be important to reveal co-associations and inform targeted extraction methods such as the reductive and/or acid dissolution of Fe/Mn phases (Senanayake, 2011; Zhang and Cheng, 2007). The REE enrichment of both Al and Mn solid phases in DLB treatment solids suggest that these are important phases for REE removal in passive CMD treatment systems.

4.3. REE partitioning in treatment solids

Total REE enrichment in treatment solids is dependent on treatment technology (e.g. LP vs DLB). However, individual REE can be uniquely partitioned into solids in mining environments (Prudêncio et al., 2015; Romero et al., 2010; Verplanck et al., 2004). In this study, REE concentrations in treatment solids (REE_S) are normalized to REE concentrations in influent CMD (REE_{IN}) to show individual REE partitioning into treatment solids (Fig. 6) (Bau, 1999). Although there is anomalously high Ce removal and anomalously low Y removal in DLBs

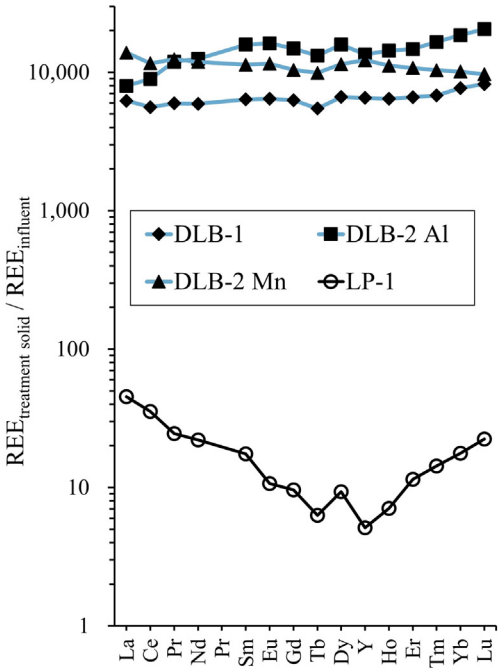

Fig. 6. REE concentrations in treatment solids (ppm) normalized to influent CMD REE concentrations (mg/L).

when comparing effluent and influent water samples (Fig. 3), corresponding positive Ce and negative Y anomalies are not observed in REE_S/REE_{IN} patterns (Fig. 6). Mass balance calculations ((REE_{IN} – REE_{OUT}) / REE_{IN}) for DLB-1, DLB-2, and DLB-3, show that the anomalous removal of Ce and Y in DLBs (Fig. 3) would result in negligible Ce and Y anomalies in corresponding treatment solids. In addition, REE concentrations in influent and effluent CMD samples are instantaneous measurements while REE concentrations in treatment solids integrate REE removal over longer, multi-season time periods complicating Ce and Y relationships between water samples and treatment solids.

The overall REE patterns in Fig. 6 show that LP-1 does not effectively concentrate REE into treatment solids, especially for middle REE, whereas DLB technologies effectively concentrate REE into treatment solids. Although both Al- and Mn-rich treatment solids from DLB-2 accumulate REE, Fig. 6 demonstrates that the Al-rich treatment solids accumulate heavy REE more effectively than the Mn-rich treatment solids. De Carlo et al. (2000) reported enhanced removal of dissolved heavy REE compared to light REE at pH < 7.5 by synthetic ferric hydroxide in marine conditions. Field observations during the excavations of operating DLBs show that treatment solids near the influent of DLBs can be white (Al-rich treatment solids) and transition to black (Mn-rich treatment solids) further from the influent. If heavy REE are also preferentially removed from CMD by Al solids at lower pH, dissolved Al and heavy REE could be preferentially co-precipitating near the influent of DLBs enriching Al solids in heavy REE.

4.4. REE concentration in different treatment systems (passive vs. active)

To complement the passive systems sampled in this study, we aggregated existing REE data from additional passive and active CMD treatment systems to determine how treatment technology may impact REE concentrations in treatment solids. We compared the performance of both passive (SP, LP, VFP, DLB) and active (lime) treatment systems by calculating REE solids concentration factors (CF_s) for each system (see methods for a complete description). For the 17 treatment systems included in this study CF_s range from 0.01 to 33 and total REE concentrations (calculated from Y concentrations) in the solids range from 88 to 2194 ppm.

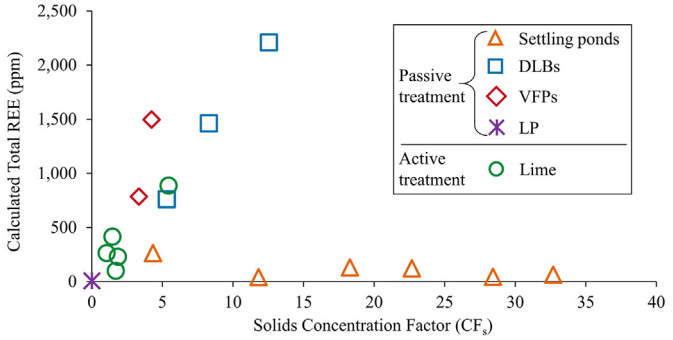

Fig. 7. Solids concentration factors (CF_s) and total REE concentrations in treatment solids produced from various CMD treatment technologies. See methods Section 2.4 for a description of CF_s. Total REE concentrations are calculated from Y concentrations using the relationship in Fig. S1. VFP data is calculated using a mass balance approach described in the methods section.

Plotting CF_s and total REE calculations suggest four groups of treatment technologies (Fig. 7): (1) LP systems with low CF_s and total REE concentrations, (2) lime (CaO, $Ca(OH)_2$) systems with low to moderate CF_s and total REE concentrations, (3) SPs with high CF_s and low total REE concentrations, and (4) DLBs and VFPs with moderate CF_s and high total REE concentrations. As discussed above, LP systems do not concentrate REE into treatment solids resulting in low CF_s and total REE concentrations. SPs have high CF_s but produce treatment solids with low total REE concentrations because this technology is primarily used to treated circumneutral CMD with low REE concentrations. DLBs, VFPs, and lime systems all utilize alkaline reagents to treat acidic influent but produce solids with markedly different REE CF_s and total REE concentrations.

The passive treatment of low-pH CMD with limestone dissolution (VFPs and DLBs) have the potential to concentrate REE into treatment solids about three times more effectively than active systems that use lime and can produce treatment solids with about three times higher REE concentrations (Fig. 7). In active treatment systems, lime addition creates a high pH, high Ca^{2+}, high SO_4^{2-}, weakly carbonate-buffered system resulting in nontargeted precipitation (e.g., calcite, gypsum, $Mg(OH)_2$). The additional precipitation, together with unreacted lime, will dilute the final REE concentrations in treatment solids from lime systems. However, limestone dissolution from passive treatment systems creates a bicarbonate-buffered system where nontargeted precipitation is minimal. Therefore, DLB and VFP systems treating low-pH, metal contaminated CMD via limestone dissolution concentrate REE most effectively in treatment solids.

4.5. CMD treatment solids as potential REE resources

High concentrations of total REE and high % critical REE in CMD treatment solids suggest they are a promising REE recovery source compared to many conventional and newly proposed REE sources. Fig. 8 shows that total and critical REE concentrations in CMD treatment solids are generally higher than US and China coals (Dai et al., 2008; Finkelman, 1993), ocean ferromanganese nodules (Bau et al., 2014), and coal fly ash (Stuckman et al., 2018) and are comparable to deep sea muds (Takaya et al., 2018). Although total REE concentrations are less than those for conventional carbonatite sources, the CMD treatment solids evaluated in this study contain an average 48% critical REE (Nd, Eu, Tb, Dy, Y) whereas carbonatites typically contain < 20% (Ault et al., 2015; Bao and Zhao, 2008; Castor, 2008; Lynas Corporation Ltd, 2012). Critical REE in CMD solids approach that of ion adsorbed clay deposits (~75%) which currently provide a substantial portion of the world's REE resources (Bao and Zhao, 2008; Dutta et al., 2016; Long et al., 2010). Additionally, treatment solids are low in radioactive elements U and Th with concentrations averaging 6.1 ppm (± 6.9 ppm)

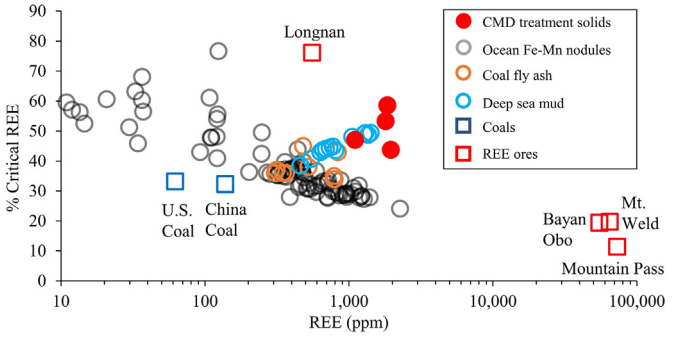

Fig. 8. Total REE concentrations vs. % critical REE (Y, Nd, Dy, Eu, Tb) for CMD treatment solids, coal fly ash (Stuckman et al., 2018), ocean Fe–Mn nodules (Bau et al., 2014), deep sea mud (Takaya et al., 2018), average U.S. and China coals (Dai et al., 2008; Finkelman, 1993), and mined ores (Ault et al., 2015; Bao and Zhao, 2008; Castor, 2008; Dutta et al., 2016; Long et al., 2010; Lynas Corporation Ltd, 2012). Longnan is an ion absorbed ore. Mountain Pass and Bayan Obo are carbonatite ores and Mt. Weld is a carbonatite laterite ore. LP-1 data not included as treatment solids from LP systems should not be targeted for REE recovery.

and 10.2 ppm (± 8.8 ppm), respectively, compared to > 300 ppm Th for some carbonatite deposits (Ault et al., 2015). High proportions of easily leachable critical REE and low radioactivity are what make small ($< 10^7$ kg of ore) ion-absorbed REE clay deposits economical to mine (Papangelakis and Moldoveanu, 2014; Wall, 2014; Yang et al., 2013). High proportions of critical REE and low radioactivity could also make CMD treatment solids attractive REE sources.

5. Conclusions

We report rare earth element data from eight passive coal mine drainage (CMD) treatment systems to determine the geochemical conditions required for REE sequestration and microanalysis work on selected CMD solids produced from these systems to identify REE-enriched phases for potential REE recovery. REE removal in passive treatment systems is pH dependent and redox independent. If pH is raised > 6.0 during the treatment process, > 90% REE are sequestered in treatment solids. Passive treatment systems using limestone to neutralize acidity can concentrate REE in treatment solids about three times more effectively than active treatment systems using lime to neutralize acidity. These limestone-based passive systems, such as drainable limestone beds and vertical flow ponds, can produce treatment solids with REE concentrations up to 1950 ppm and with up to 55% energy critical REE and 56% middle and heavy REE. Both Al- and Mn-rich treatment solids produced from passive systems can be enriched in REE and in Mn-rich treatment solids, REE are diffusely distributed in the Mn-rich layer cemented onto limestone aggregate. CMD treatment solids can contain higher REE concentrations and higher % critical REE compared to many other novel REE sources (e.g., ocean Fe–Mn nodules, coal fly ash, deep sea muds, and coal) and this study indicates that REE in CMD treatment solids represent a substantial REE recovery opportunity. The recovery of REE from treatment solids is an opportunity to transform mine drainage, an environmental challenge and economic liability, into an asset, further spurring the treatment of polluted water.

Acknowledgements

This research was supported by a University of Pittsburgh Mellon Predoctoral Fellowship, the Dr. J. Frederick and Ann Sarg Research Award from The University of Pittsburgh's Geology and Environmental Science Department, a CRDF grant from the University of Pittsburgh (RCC), logistical support and data from Hedin Environmental, and an appointment by the U.S. Department of Energy (DOE) Postgraduate Research Program at the National Energy Technology Laboratory administered by the Oak Ridge Institute for Science and Education (ORISE). The synchrotron work was conducted on beamline 2-3 at the Stanford Synchrotron Radiation Lightsource, SLAC national Accelerator laboratory, which is supported by the U.S. Department of Energy, Office of Sciences, Office of Basic Energy Sciences under Contract No. DE-AC02-76SF00515. We thank Dr. Charles Cravotta III for sharing data and for a detailed review of an earlier version of this manuscript. The manuscript was improved by comments and suggestions from Dennis Kraemer and an anonymous reviewer. We also thank Dr. Wei Xiong (NETL) for her aid in SEM analyses. Use of trade, firm, or product names is for descriptive purposes only and does not imply endorsement by the U.S. Government.

Appendix A. Supplementary data

Supplementary data to this article can be found online at https://doi.org/10.1016/j.coal.2019.04.007.

References

Actlabs, 2018. Methods. Retrieved from. http://www.actlabs.com/list.aspx?menu=64&app=226&cat1=549&tp=12&lk=no.

Alonso, E., Sherman, A.M., Wallington, T.J., Everson, M.P., Field, F.R., Roth, R., Kirchain, R.E., 2012. Evaluating rare earth element availability: a case with revolutionary demand from clean technologies. Environ. Sci. Technol. 46 (6), 3406–3414. https://doi.org/10.1021/es203518d.

Ault, T., Krahn, S., Croff, A., 2015. Radiological Impacts and Regulation of rare Earth elements in Non-Nuclear Energy Production. Energies 8 (3), 2066–2081. https://doi.org/10.3390/en8032066.

Ayora, C., Macias, F., Torres, E., Lozano, A., Carrero, S., Nieto, J.M., Perez-Lopez, R., Fernandez-Martinez, A., Castillo-Michel, H., 2016. Recovery of rare Earth elements and Yttrium from Passive-Remediation Systems of Acid Mine Drainage. Environ. Sci. Technol. 50 (15), 8255–8262. https://doi.org/10.1021/acs.est.6b02084.

Bao, Z., Zhao, Z., 2008. Geochemistry of mineralization with exchangeable REY in the weathering crusts of granitic rocks in South China. Ore Geol. Rev. 33 (3–4), 519–535. https://doi.org/10.1016/j.oregeorev.2007.03.005.

Bau, M., 1999. Scavenging of dissolved yttrium and rare earths by precipitating iron oxyhydroxide: Experimental evidence for Ce oxidation, Y-Ho fractionation, and lanthanide tetrad effect. Geochim. Cosmochim. Acta 63 (1), 66–77.

Bau, M., Koschinsky, A., 2009. Oxidative scavenging of cerium of hydrous Fe oxide: evidence from the distribution of rare earth elements and yttrium between Fe oxides and Mn oxides in hydrogenetic ferromanganese crusts. Geochem. J. 43, 37–47.

Bau, M., Koschinsky, A., Dulski, P., Hein, J., 1996a. Comparison of the partitioning behaviors of yttrium, rare earth elemtns, and titanium between hydrogenetic marine ferromanganese crusts and seawater. Geochim. Cosmochim. Acta 60 (10), 1709–1725.

Bau, M., Koschinsky, A., Dulski, P., Hein, J., 1996b. Comparison of the partitioning behaviours of yttrium, rare earth elements, and titanium between hydrogenetic marine ferromanganese crusts and seawater. Geochim. Cosmochim. Acta 60 (10), 1709–1725.

Bau, M., Schmidt, K., Koschinsky, A., Hein, J., Kuhn, T., Usui, A., 2014. Discriminating between different genetic types of marine ferro-manganese crusts and nodules based on rare earth elements and yttrium. Chem. Geol. 381, 1–9. https://doi.org/10.1016/j.chemgeo.2014.05.004.

Bigham, J.M., Schwertmann, U., Traina, S.J., Winland, R.L., Wolf, M., 1996. Schwertmannite and the chemical modeling of iron in acid sulfate waters. Geochim. Cosmochim. Acta 60 (12), 2111–2121.

Binnemans, K., Jones, P.T., Blanpain, B., Van Gerven, T., Yang, Y., Walton, A., Buchert, M., 2013. Recycling of rare earths: a critical review. J. Clean. Prod. 51, 1–22. https://doi.org/10.1016/j.jclepro.2012.12.037.

Cao, X., Chen, Y., Wang, X., Deng, X., 2001. Effects of redox potential and pH value on the release of rare earth elements from soil. Chemosphere 44 (4), 655–661.

Castor, S.B., 2008. The Mountain Pass Rare-Earth Carbonatite and Associated Ultrapotassic Rocks, California. Can. Mineral. 46, 779–806. https://doi.org/10.3749/canmin.46.4.779.

Cavazza, E.C., Beam, R.L., 2010. Restoring the Bennett Branch Sinnemahoning Creek, Clearfield and Elk Counties, Pennsylvania. In: Paper Presented at the 2010 National Meeting of the American Society of Mining and Reclamation, Pittsburgh, PA, USA.

Cravotta, C.A., 2008. Dissolved metals and associated constituents in abandoned coal-mine discharges, Pennsylvania, USA. Part 1: constituent quantities and correlations. Appl. Geochem. 23 (2), 166–202. https://doi.org/10.1016/j.apgeochem.2007.10.011.

Cravotta, C.A., Brady, K.B.C., 2015. Priority pollutants and associated constituents in untreated and treated discharges from coal mining or processing facilities in Pennsylvania, USA. Appl. Geochem. 62, 108–130. https://doi.org/10.1016/j.apgeochem.2015.03.001.

Cravotta, C.A., Trahan, M.K., 1999. Limestone drains to increase pH and remove dissolved metals from acidic mine drainage. Appl. Geochem. 14, 581–606.

Dai, S., Finkelman, R.B., 2018. Coal as a promising source of critical elements: progress and future prospects. Int. J. Coal Geol. 186, 155–164. https://doi.org/10.1016/j.coal.2017.06.005.
Dai, S., Li, D., Chou, C.-L., Zhao, L., Zhang, Y., Ren, D., Ma, Y., Sun, Y., 2008. Mineralogy and geochemistry of boehmite-rich coals: new insights from the Haerwusu Surface Mine, Jungar Coalfield, Inner Mongolia, China. Int. J. Coal Geol. 74 (3–4), 185–202. https://doi.org/10.1016/j.coal.2008.01.001.
Davranche, M., Pourret, O., Gruau, G., Dia, A., 2004. Impact of humate complexation on the adsorption of REE onto Fe oxyhydroxide. J. Colloid Interface Sci. 277 (2), 271–279. https://doi.org/10.1016/j.jcis.2004.04.007.
Davranche, M., Pourret, O., Gruau, G., Dia, A., Jin, D., Gaertner, D., 2008. Competitive binding of REE to humic acid and manganese oxide: impact of reaction kinetics on development of cerium anomaly and REE adsorption. Chem. Geol. 247, 154–170. https://doi.org/10.1016/j.chemgeo.2007.10.010.
de Carlo, E.H., Wen, X.-Y., Irving, M., 1998. The Influence of Redox Reactions on the Uptake of Dissolved Ce by Suspended Fe and Mn Oxide Particles. Aquat. Geochem. 3, 357–389.
De Carlo, E.H., Wen, X.Y., Cowen, J.P., 2000. Rare earth element fractionation in Hydrogenetic Fe-Mn Crusts: the influence of carbonate complexation and phosphatization on Sm/Yb Ratios. In: Marine Authigenesis: From Global to Microbial, pp. 271–285.
DeSa, T.C., Brown, J.F., Burgos, W.D., 2010. Laboratory and Field-scale Evaluation of low-pH Fe(II) Oxidation at Hughes Borehole, Portage, Pennsylvania. Mine Water Environ. 29 (4), 239–247. https://doi.org/10.1007/s10230-010-0105-5.
DOE, 2011. U.S. Department of Energy Critical Materials Strategy. United States Department of Energy, Washington, D.C.
Du, X., Graedel, T.E., 2011. Global in-use stocks of the rare Earth elements: a first estimate. Environ. Sci. Technol. 45 (9), 4096–4101. https://doi.org/10.1021/es102836s.
Dutta, T., Kim, K.H., Uchimiya, M., Kwon, E.E., Jeon, B.H., Deep, A., Yun, S.T., 2016. Global demand for rare earth resources and strategies for green mining. Environ. Res. 150, 182–190. https://doi.org/10.1016/j.envres.2016.05.052.
EPA. (2015, March 3, 2017). 303(d) List Impaired Waters NHDPlus Indexed Dataset with Program Attributes. May 1, 2015. Retrieved from https://www.epa.gov/waterdata/waters-geospatial-data-downloads
Erickson, B., 2018. Rare-earth Recovery. Chem. Eng. News 96, 28–33 7/9/2018.
Finkelman, R.B., 1993. Trace and Minor elements in coal. In: Organic Geochemistry, pp. 593–607.
Gromet, L.P., Dymek, R.F., Haskin, L.A., Korotev, R.L., 1984. The "north American shale composite": its compilation, major and trace element characteristics. Geochim. Cosmochim. Acta 48, 2469–2482.
Hansel, C.M., Zeiner, C.A., Santelli, C.M., Webb, S.M., 2012. Mn(II) oxidation by an ascomycete fungus is linked to superoxide production during asexual reproduction. Proc. Natl. Acad. Sci. U. S. A. 109 (31), 12621–12625. https://doi.org/10.1073/pnas.1203885109.
Haque, N., Hughes, A., Lim, S., Vernon, C., 2014. Rare Earth elements: Overview of Mining, Mineralogy, Uses, Sustainability and Environmental Impact. Resources 3 (4), 614–635. https://doi.org/10.3390/resources3040614.
Haskin, M.A., Haskin, L.A., 1966. Rare earths in european shales: a redetermination. Science 154, 507–509.
Hedin, R.S., 2003. Recovery of marketable iron oxide from mine drainage in the USA. Land Contam. Reclam. 11 (2), 93–97. https://doi.org/10.2462/09670513.802.
Hedin, R.S., 2008. Iron removal by a passive system treating alkaline coal mine drainage. Mine Water Environ. 27 (4), 200–209. https://doi.org/10.1007/s10230-008-0041-9.
Hedin Environmental, 2008. Optimizing the Design and Operation of Self-Flushing Limestone Systems for Mine Drainage Treatment. Retrieved from. http://files.dep.state.pa.us/Mining/Abandoned%20Mine%20Reclamation/AbandonedMinePortalFiles/InnovativeTechnologyGrantFinalReports/Flushing.pdf.
Hedin, R.S., Watzlaf, G.R., Nairn, R.W., 1994. Passive treatment of acid mine drainage with limestone. J. Environ. Qual. 23, 1338–1345.
Hedin, R., Weaver, T., Wolfe, N., Weaver, K., 2010. Passive treatment of acidic coal mine drainage: the anna s mine passive treatment complex. Mine Water Environ. 29 (3), 165–175. https://doi.org/10.1007/s10230-010-0117-1.
Hedin, R., Weaver, T., Wolfe, N., Watzlaf, G., 2013. Effective Passive Treatment of Coal Mine Drainage. In: Paper Presented at the 35th Annual National Association of Abandoned Mine Land Programs Conference. The Resort at Glade Springs, Daniels, West Virginia.
Hein, J.R., Mizell, K., Koschinsky, A., Conrad, T.A., 2013. Deep-ocean mineral deposits as a source of critical metals for high- and green-technology applications: comparison with land-based resources. Ore Geol. Rev. 51, 1–14. https://doi.org/10.1016/j.oregeorev.2012.12.001.
Hudson-Edwards, K.A., Jamieson, H.E., Lottermoser, B.G., 2011. Mine Wastes: past, Present, Future. Elements 7 (6), 375–380. https://doi.org/10.2113/gselements.7.6.375.
Kairies, C.L., Capo, R.C., Watzlaf, G.R., 2005. Chemical and physical properties of iron hydroxide precipitates associated with passively treated coal mine drainage in the Bituminous Region of Pennsylvania and Maryland. Appl. Geochem. 20 (8), 1445–1460. https://doi.org/10.1016/j.apgeochem.2005.04.009.
Koschinsky, A., Heinrich, L., Boehnke, K., Cohrs, J.C., Markus, T., Shani, M., Singh, P., Smith Stegen, K., Werner, W., 2018. Deep-sea mining: interdisciplinary research on potential environmental, legal, economic, and societal implications. Integr. Environ. Assess. Manag. https://doi.org/10.1002/ieam.4071.
Larson, L.N., Sánchez-España, J., Burgos, W., 2014. Rates of low-pH biological Fe(II) oxidation in the Appalachian Bituminous Coal Basin and the Iberian Pyrite Belt. Appl. Geochem. 47, 85–98. https://doi.org/10.1016/j.apgeochem.2014.05.012.
Lin, R., Stuckman, M., Howard, B.H., Bank, T.L., Roth, E.A., Macala, M.K., Lopano, C., Soong, Y., Granite, E.J., 2018. Application of sequential extraction and hydrothermal treatment for characterization and enrichment of rare earth elements from coal fly ash. Fuel 232, 124–133. https://doi.org/10.1016/j.fuel.2018.05.141.
Liu, H., Pourretc, O., Guoa, H., Bonhourec, J., 2017. Rare earth elements sorption to iron oxyhydroxide: model development and application to groundwater. Appl. Geochem. 87, 158–166. https://doi.org/10.1016/j.apgeochem.2017.10.020.
Long, K.R., Gosen, B.S.V., Foley, N.K., Cordier, D., 2010. The Principal Rare Earth Element Deposits of the United States—A Summary of Domestic Deposits and a Global Perspective (Retrieved from Available at). http://pubs.usgs.gov/sir/2010/5220/.
Luan, F., Santelli, C.M., Hansel, C.M., Burgos, W.D., 2012. Defining manganese(II) removal processes in passive coal mine drainage treatment systems through laboratory incubation experiments. Appl. Geochem. 27 (8), 1567–1578. https://doi.org/10.1016/j.apgeochem.2012.03.010.
Lynas Corporation Ltd, 2012. Increase in Mt Weld Resource Estimate for the Central Lanthanide Deposit and Duncan Deposit. (Retrieved from 56 Pitt Street Sydney NSW 2000).
Margolis, S.V., Burns, R.G., 1976. Pacific Deep-Sea Manganese Nodules: their distribution, Composition, and Origin. Annu. Rev. Earth Planet. Sci. 4, 229–263.
Montross, S.N., Verba, C.A., Chan, H.L., Lopano, C., 2018. Advanced characterization of rare earth element minerals in coal utilization byproducts using multimodal image analysis. Int. J. Coal Geol. 195, 362–372. https://doi.org/10.1016/j.coal.2018.06.018.
Noack, C.W., Dzombak, D.A., Karamalidis, A.K., 2014. Rare earth element distributions and trends in natural waters with a focus on groundwater. Environ. Sci. Technol. 48 (8), 4317–4326. https://doi.org/10.1021/es4053895.
Ohta, A., Kawabe, I., 2001. REE(III) adsorption onto Mn dioxide (d-MnO2) and Fe oxyhydroxide: Ce(III) oxidation by d-MnO2. Geochim. Cosmochim. Acta 65 (5), 695–703.
Papangelakis, V.G., Moldoveanu, G., 2014. Recovery of rare Earth elements from Clay Minerals. In: Paper Presented at the ERES 2014 — The 1st Conference on European Rare Earth Resources, Milos, Greece.
Post, J.E., 1999. Manganese oxide minerals: Crystal structures and economic and environmental significance. Proc. Natl. Acad. Sci. U. S. A. 96, 3447–3454.
Pourret, O., Martinez, R.E., 2009. Modeling lanthanide series binding sites on humic acid. J. Colloid Interface Sci. 330 (1), 45–50. https://doi.org/10.1016/j.jcis.2008.10.048.
Prudêncio, M.I., Valente, T., Marques, R., Braga, M.A.S., 2015. Geochemistry of rare earth elements in a passive treatment system built for acid mine drainage remediation. Chemosphere 138, 691–700. https://doi.org/10.1016/j.chemosphere.2015.07.064.
Pu, X., Vazquez, O., Monnell, J.D., Neufeld, R.D., 2010. Speciation of Aluminum precipitates from acid rock discharges in Central Pennsylvania. Environ. Eng. Sci. 27 (2), 169–180.
Romero, F.M., Prol-Ledesma, R.M., Canet, C., Alvares, L.N., Pérez-Vázquez, R., 2010. Acid drainage at the inactive Santa Lucia mine, western Cuba: natural attenuation of arsenic, barium and lead, and geochemical behavior of rare earth elements. Appl. Geochem. 25, 716–727. https://doi.org/10.1016/j.apgeochem.2010.02.004.
Santelli, C.M., Webb, S.M., Dohnalkova, A.C., Hansel, C.M., 2011. Diversity of Mn oxides produced by Mn(II)-oxidizing fungi. Geochim. Cosmochim. Acta 75 (10), 2762–2776. https://doi.org/10.1016/j.gca.2011.02.022.
Schwertmann, U., Carlson, L., 2005. The pH-dependent transformation of schwertmannite to goethite at 25C. Clay Miner. 40, 63–66.
Senanayake, G., 2011. Acid leaching of metals from deep-sea manganese nodules – a critical review of fundamentals and applications. Miner. Eng. 24 (13), 1379–1396. https://doi.org/10.1016/j.mineng.2011.06.003.
Seredin, V.V., Dai, S., 2012. Coal deposits as potential alternative sources for lanthanides and yttrium. Int. J. Coal Geol. 94, 67–93. https://doi.org/10.1016/j.coal.2011.11.001.
Skousen, J.G., Zipper, C.E., Rose, A., Ziemkiewicz, P.F., Nairn, R.W., McDonald, L.M., Kleinmann, R.L., 2017. Review of passive systems for acid mine drainage treatment. Mine Water Environ. 36, 133–153. https://doi.org/10.1007/s10230-016-0417-1.
Stewart, B.W., Capo, R.C., Hedin, B.C., Hedin, R.S., 2017. Rare earth element resources in coal mine drainage and treatment precipitates in the Appalachian Basin, USA. Int. J. Coal Geol. 169, 28–39. https://doi.org/10.1016/j.coal.2016.11.002.
Stream Restoration, I, 2018. Datashed. Retrieved from. https://www.datashed.org/.
Stuckman, M.Y., Lopano, C.L., Granite, E.J., 2018. Distribution and speciation of rare earth elements in coal combustion by-products via synchrotron microscopy and spectroscopy. Int. J. Coal Geol. 195, 125–138. https://doi.org/10.1016/j.coal.2018.06.001.
Takaya, Y., Yasukawa, K., Kawasaki, T., Fujinaga, K., Ohta, J., Usui, Y., Nakamura, K., Kimura, J.I., Chang, Q., Hamada, M., Dodbiba, G., Nozaki, T., Iijima, K., Morisawa, T., Kuwahara, T., Ishida, Y., Ichimura, T., Kitazume, M., Fujita, T., Kato, Y., 2018. The tremendous potential of deep-sea mud as a source of rare-earth elements. Sci. Rep. 8 (1), 5763. https://doi.org/10.1038/s41598-018-23948-5.
Tan, H., Zhang, G., Heaney, P.J., Webb, S.M., Burgos, W.D., 2010. Characterization of manganese oxide precipitates from Appalachian coal mine drainage treatment systems. Appl. Geochem. 25 (3), 389–399. https://doi.org/10.1016/j.apgeochem.2009.12.006.
USGS, 2018. Mineral Commodity Summaries: Rare Earths. United Stated Department of the Interior, United States Geological Survey, Reston, Virginia.
Verplanck, P.L., Nordstrom, D.K., Taylor, H.E., Kimball, B.A., 2004. Rare earth element partitioning between hydrous ferric oxides and acid mine water during iron oxidation. Appl. Geochem. 19 (8), 1339–1354. https://doi.org/10.1016/j.apgeochem.2004.01.016.
Vesper, D.J., Smilley, M.J., 2010. Attenuation and diel cycling of coal-mine drainage constituents in a passive treatment wetland: a case study from Lambert Run, West Virginia, USA. Appl. Geochem. 25 (6), 795–808. https://doi.org/10.1016/j.apgeochem.2010.02.010.

Wall, F., 2014. Rare Earth elements. In: Gunn, G. (Ed.), Critical Metals Handbook. John Wiley & Sons, Ltd.
Webb, S.M., 2005. SIXpack: a graphical user interface for XAS analysis using IFEFFIT. Phys. Scr. 2005, 1011–1014.
Yang, X.J., Lin, A., Li, X.-L., Wu, Y., Zhou, W., Chen, Z., 2013. China's ion-adsorption rare earth resources, mining consequences and preservation. Environ. Dev. 8, 131–136. https://doi.org/10.1016/j.envdev.2013.03.006.
Younger, P.L., Banwart, S.A., Hedin, R.S., 2002. Mine Water: Hydrology, Pollution, Remediation. Kluwer Academic Publishers, Norwell, MA.
Zhang, W., Cheng, C.Y., 2007. Manganese metallurgy review. Part I: leaching of ores/secondary materials and recovery of electrolytic/chemical manganese dioxide. Hydrometallurgy 89 (3–4), 137–159. https://doi.org/10.1016/j.hydromet.2007.08.010.
Zhang, W., Honaker, R.Q., 2018. Rare earth elements recovery using staged precipitation from a leachate generated from coarse coal refuse. Int. J. Coal Geol. 195, 189–199. https://doi.org/10.1016/j.coal.2018.06.008.
Zhou, B., Li, Z., Chen, C., 2017. Global potential of rare Earth Resources and rare Earth demand from Clean Technologies. Minerals 7 (11). https://doi.org/10.3390/min7110203.
Ziemkiewicz, P., He, T., Noble, A., Lui, X., 2016. Recovery of rare Earth elements (REEs) from Coal Mine Drainage. In: Paper Presented at the West Virginia Mine Drainage Task Force, Morgantown, WV.